ACS APPLIED MATERIALS & INTERFACES

Research Article

www.acsami.org

Enhanced Epoxy/Silica Composites Mechanical Properties by Introducing Graphene Oxide to the Interface

Li Chen,[†] Songgang Chai,[‡] Kai Liu,[†] Nanying Ning,[†] Jian Gao,[†] Qianfa Liu,[‡] Feng Chen,*[,†] and Qiang Fu*[,†]

[†]College of Polymer Science and Engineering, State Key Laboratory of Polymer Materials Engineering, Sichuan University, Chengdu 610065, China

[‡]Guangdong Shengyi Technology Limited Corporation, Dongguan, 523039, China

ABSTRACT: Controlling the interface interaction of polymer/filler is essential for the fabrication of high-performance polymer composites. In this work, a core−shell structured hybrid (SiO_2−GO) was prepared and introduced into an epoxy polymer matrix as a new filler. The incorporation of the hybrid optimized the modulus, strength and fracture toughness of the composites simultaneously. The ultrathin GO shells coated on silica surfaces were regarded as the main reason for the enhancement. Located at the silica-epoxy interface, GO served as an unconventional coupling agent of the silica filler, which effectively enhanced the interfacial interaction of the epoxy/SiO_2−GO composites, and thus greatly improved the mechanical properties of the epoxy resin. We believe this new and effective approach that using GO as a novel fillers surface modifier may open a novel interface design strategy for developing high performance composites.

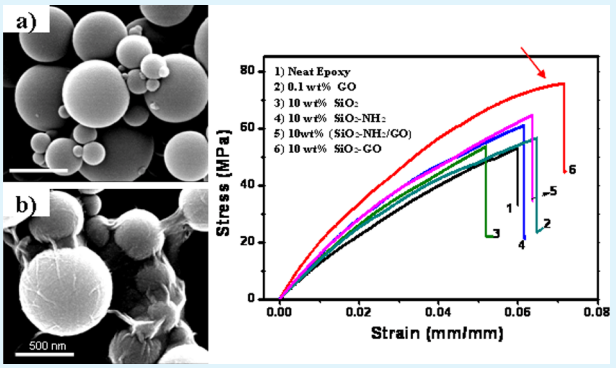

KEYWORDS: *graphene oxide, epoxy, core−shell structure, interfacial enhancement*

1. INTRODUCTION

Polymer/inorganic filler composites have attracted considerable scientific and industrial interest over the past few decades. The combined advantages of inorganic material and polymer usually afford polymer composites with unique performances.[1−4] For instance, in the microelectronics industries, epoxy/silica composites have been used widely as electronics packaging materials. Where silica particles are introduced to epoxy resin for reducing the coefficients of thermal expansion (CTE), lowering shrinkage on curing and mechanical reinforcement.[5−8] To prepare high-performance polymer composites, the dispersion of inorganic fillers and the interfacial interaction between matrix and fillers are considered as the key issues. The fillers/matrix interfacial cohesion directly influence the interfacial stess transfer in the composites structures, thereby signifcantly affects the integrated mechanical properties. In recent decades, great efforts have been made by scientists and engineers to improve the interfacial adhesion in polymer composites. Various methods have been used to enhance the interfacial interaction, and a particular attention has been focused on either enhancing the chemical activity of the fillers surface or increasing the surface area.[9−13]

Graphene oxide (GO) nanosheets are heavily oxygenated graphene, which can be easily acquired from natural graphite flakes by strong oxidation and subsequent exfoliation.[14,15] With a great deal of epoxy, hydroxyl, and carboxyl functional groups on its basal planes, GO can be stably dispersed in water, these functional groups also make it more compatible with organic polymers. For this reason, GO has attracted considerable attention as an ideal two-dimensional reinforcing component for polymers.[16−20] While, the unique and superior properties of GO for material applications continue to be recognized or discovered. Recent studies demonstrated that each GO sheet can be regarded as a colloidal particle as well as a single molecule, this "soft" two-dimensional macromolecule behavior makes it feasible to assemble from microstructure to well-defined hierarchical structures via certain interactions.[21−27] In particular, taking advantage of the negatively charged surface, GO can coassemble with some positively charged particles via mutual electrostatic interaction. Several GO (graphene) encapsulated core−shell hybrids were fabricated by this novel electrostatic self-assembly strategy.[23−25] The coated ultrathin GO (graphene) on organic/inorganic objects always endowed them special properties and applications.[23−27]

In this work, taking the advantage of the unique structure and properties of GO nanosheets, we develop a new and effective strategy for improving the polymer/fillers interfacial adhesions. A core−shell structured hybrid with ultrathin GO shells on silica surface (SiO_2−GO) was fabricated and introduced into a thermoset polymer, the epoxy resin, and its potential application as reinforcement for polymer composites were studied. Results showed that the incorporation of SiO_2−

Received: June 14, 2012
Accepted: August 2, 2012
Published: August 2, 2012

GO hybrid significantly improved composites mechanical properties, the mechanical reinforcement efficacy of SiO_2−GO is far better than that of other fillers compared. Locating at the filler/matrix interface, the ultrathin GO are preferable to traditional coupling agent for the enhancement of silica−epoxy interfacial adhesion.

2. EXPERIMENTAL SECTION

2.1. Materials. Graphite powders were purchased from Qingdao Black Dragon graphite Co., Ltd. Submicro sized silica (average diameter: 400 nm) was supplied by Guangdong Shengyi Technology Co., LTD (China).The epoxy resin, diglycidyl ether of biphenol A epoxy EPON 828, was obtained from Shell Chemicals. This resin was used in combination with the commercial aromatic diamine 4,4′-methylene bis(2,6-diethylaniline (MDEA, Changzhou Xinghui Chemical Co., Ltd.) as a curing agent. Potassium permanganate ($KMnO_4$), sulfuric acid (H_2SO_4 98%), hydrogen peroxide (H_2O_2), hydrochloric acid and tetrahydrofuran (THF), 3-aminopropyltriethoxysilane (APS) were purchased from Kelong Chemical reagent plant (Chengdu, China), all reagents were used as received.

2.2. Fabrication of Core−Shell Structured SiO_2−GO Hybrid. Similar to previous studies,[25] the core−shell structured SiO_2−GO hybrid were prepared by the simply two steps: the modification of silica particles with APS coupling agent, and the surface assembly of GO nanosheets with the modified silica microsperes.

GO was prepared from natural graphite by Hummers method.[14] Exfoliation of GO was achieved by sonication for 2 h in an aqueous solvent, the nonexfoliated GO sheets were removed by centrifuged. The surface modification of SiO_2 with APS coupling agent was carried out in liquid phase. In a typical process, SiO_2 powder (10 g) was first dispersed well in 300 mL of ethanol, added with 0.5 mL of silane coupling agent APS. The mixture was stirred and kept at 323 K for 12 h, then the grafting reaction was realized, the obtain SiO_2−NH_2 particles were filtered from the mixture, washed with ethanol and deionized water five times, and dried under vacuum.

The SiO_2−GO hybrid was fabricated simply by mixing the neutral aqueous suspension of SiO_2−NH_2 and GO solution. 400 mL SiO_2−NH_2 suspension (20 mg/mL) was added into a 400 mL aqueous GO solution (0.2 mg/mL) under mild magnetic stirring for 1 h. When stirring stopped, the GO precipitated with SiO_2−NH_2 at the bottom of the beaker. The sediment solid (SiO_2−GO) was collected and washed with water several times to remove the unbound GO, then freeze-dried under vacuum.

2.3. Preparation of Epoxy-Based Composites. For the preparation of epoxy/SiO_2−GO composites, the desired amount of SiO_2−GO was dispersed in THF solvent with a high-shear mixer and ultrasonic treatment, and then mixed with predetermined amount of epoxy oligomer with stirring for 1 h. Next, the solvent was evaporated off by heating the mixture on a magnetic stir plate at 70 °C for 2 h, and further degassed overnight in a vacuum oven. After that, a stoichiometric amount of amine curing agent was added to the mixture, the ingredients were mixed for 1 h at 60 °C, and degassed in a vacuum oven for 2 h at 70 °C to remove the residual solvent. The mixture was poured into a preheated mold, cured at 120 °C for 3 h, at 180 °C for 3 h. Neat epoxy resin, composites samples loaded with other fillers were also prepared by the same procedure.

2.4. Characterization. SEM images were obtained on a FEI Inspect F scanning electron microscopy (SEM) instrument. Tests of fracture surfaces microscopic morphology were also conducted on a FESEM under an acceleration voltage of 15 kV, all samples were fractured at room temperature. The morphology and structure of the resulting SiO_2−GO hybrid were also elucidated by high-resolution TEM (TEM, Tecnai F20 S-TWIN) measurements.

The FT-IR spectra were recorded between 400 and 4000 cm^{-1} on a Nicolet-560 infrared spectrometer. XPS measurements (Axis Ultra DLD, Kratos, UK) was performed using focused monochromatized Al Kα radiation (15KV) in order to demonstrate the variation in the ratios of GO, SiO_2−NH_2 and SiO_2−GO. Raman spectra of GO and SiO_2−GO dried powder samples were obtained using a multichannel confocal micro spectrometer with a laser wavelength of 535 nm. Zeta potential measurements were performed using a Zetasizer 3000 (Malvern Instruments), the GO and silica aqueous suspensions were diluted to 0.05, 2 mg/mL, respectively, before measurements.

The tensile dumbbell samples were made using a stainless steel mold, with dimensions of 100.0 mm * 13.0 mm * 4.5 mm in the working section. An Instron universal testing machine was used to evaluate the tensile properties under a crosshead speed of 2 mm/min^{-1}. Five samples were used for each measurement and the reported results represent an average result. DMA of both neat epoxy and composite were performed with Dynamic Mechanical Analyzer (TA Instruments, USA) to determine their thermomechanical properties. The experiments were carried out on samples (30 mm × 8 mm × 3 mm) under single cantilever mode. Tests were performed at a frequency of 1 Hz with a temperature sweep from 50 to 300 °C at a ramp rate of 3 °C/min, a total of 3 tests were performed for each batch of material.

3. RESULTS AND DISCUSSION

3.1. Self-Assembly of GO and APS-Treated Silica. The GO nanosheets are negatively charged in aqueous solution, originated from the ionization of the carboxylic acid groups on their surface. When GO mixed with other positively charged particles, the mutual assembly can be triggered by the electrostatic force.[22−25] Here, the SiO_2 was first modified by APS, which could be ionization of amino groups to form positively charged SiO_2−NH_2 particles.[25] The surface charges of GO, SiO_2 and SiO_2−NH_2 in aqueous suspensions were examined by zeta potential tests. With pH value of 7.0, the GO had a highly negative surface charge withζpotential value of −39.6 mV. Meanwhile, the surface charges of the silica switched from negative (ζ potential = −25.6 mV) to positive (ζ potential = 42.2 mV) after APS modification. The grafting and the protonate effect of amino groups on the SiO_2−NH_2 particles surface make them positively charged. When the oppositely charged GO nanosheets and SiO_2−NH_2 particles met through a simple solution mixing, the electrostatic assembly might be triggered, forming the core−shell structure of GO-SiO_2 hybrid afterward.

The morphology and structure of the resultant SiO_2−GO hybrid with 1 wt % GO were elucidated by SEM and high-resolution TEM measurements (Figure 1b, c). Compared with the SiO_2 particles with a microspheres morphology and smooth surface (Figure 1a), one clearly observes that the silica surfaces are intimately covered by ultrathin GO as shown in Figure 1b. The creases and roughened textures are associated with the presence of flexible and ultrathin GO sheets. The typical HRTEM images of SiO_2−GO hybrid (Figure 1c,d) also confirm that the flexible and ultrathin GO sheets have indeed successfully wrapped around the SiO_2−NH_2 microspheres, with the GO shells thicknesses less than 3 nm. Considering the large specific surface areas gap between GO and silica, (the specific surface area of an individual GO sheet is 2,600 m^2/g), it is easy to understand why only 1 wt % GO is needed to assemble on the silica surface when the equilibrium coverage is reached.

The covalently attached APS silane coupling agent and the GO wrapping on the silica surface can be also confirmed by FT-IR and X-ray photoelectron spectroscopy (XPS) tests. As the FT-IR spectra curves of Figure 2a shows, the main peaks of SiO_2 spectra curve at 798, 1100,1640 and 3450 cm^{-1} are designed as bending vibration of SiO−H, stretching vibration of Si−OH, stretching vibration of Si−O−Si, bending vibration of O−H and stretching vibration of −OH, respectively. Several minor bands at around 2800 to 3000 cm^{-1} were detected in the

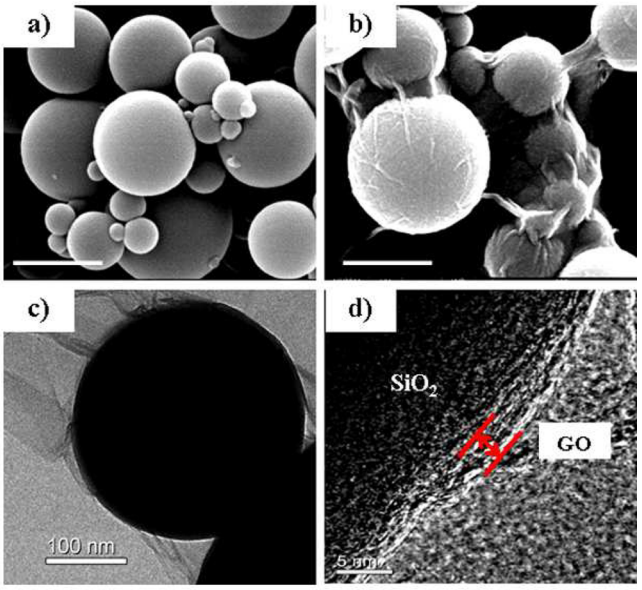

Figure 1. SEM images of the (a) raw SiO_2 and (b) created SiO_2−GO hybrid, scale bar 500 nm. (c) Transmission electron microscopy (TEM) image of a typical core−shell structured SiO_2−GO hybrid; (d) high-resolution TEM (HRTEM) images of graphene encapsulating silica spheres.

spectra of SiO_2−NH_2, which were attributed to the C−H stretching vibration of the hydrocarbon chains of the grafting APS. A weak band at 1710 cm^{-1} appeared in the SiO_2−GO spectra curve, which is the characteristic of C═O stretching vibration band of GO. As GO has a large amount of −OH groups, the peak at 3450 $cm^{-1}$of SiO_2−GO is higher than that of SiO_2−NH_2. Moreover, Table 1 shows the XPS results of the chemical compositions of GO, SiO_2−NH_2, and the SiO_2−GO hybrid. The 3.57% of nitrogen content of the SiO_2−NH_2 measured suggests a successful introduction of amino groups. A rise of carbon content from 4.00% of SiO_2−NH_2 to 24.83% of SiO_2−GO also indicates the immobilization of GO on the silica.

In addition, Raman spectroscopy, which has been utilized as a powerful tool for the characterization of graphene and its derivatives, was employed to further identify the GO shells of the SiO_2−GO hybrid. From Figure.2b, it is interesting to find that the intensities of the D and G bands are obviously increased in comparison with those of the original GO under

Table 1. Elemental Analysis Results of GO, SiO_2−NH_2, and SiO_2−GO

	relative atomic percentage (%)			
samples	C	Si	O	N
GO	67.75		32.25	
SiO_2−NH_2	4.00	31.87	60.56	3.57
SiO_2−GO	24.83	20.45	52.61	2.11

the same test conditions, although the content of GO is only 1 wt % of the SiO_2−GO hybrid. The surface-enhanced Raman scattering (SERS) effect of graphene also found in several instances.[28−30] We deduced that the ultrathin GO sheets on silica microspheres surface lead to the enhancement of Raman intensity, the precise origin is still under study. It is reported that both G and 2D bands can be used to monitor the number of layers. The G peak position of the single-layer graphene shifts to lower wavenumbers, and the 2D band decreases in intensity and lower frequency peaks after stacking more graphene layers.[31−33] In this work, the peak positions of the G bands of the mutilayers GO and SiO_2−GO were found to be centered at about 1591 and 1598 cm^{-1}, respectively. This result indicates that SiO_2−GO contains less layers compared to original GO. Moreover, compared with GO, the 2D band of SiO_2−GO is narrower and more intense, and it is downshifted from 2721 cm^{-1} of GO to 2710 cm^{-1}. Again, this result suggests that only a few layers of GO coated on the silica surface. Raman spectra result agrees well with TEM observation.

3.2. Mechanical Behavior of Epoxy Composites. Considering the SiO_2−GO hybrid, the ultrathin GO shells provide it with rough and wrinkled surface topology, and the abundant functional groups of GO can also make it more compatible with some polymers, which may create some new and exciting possibilities for the application in the field of structural materials. Herein, we explored its application as polymer reinforcement by introducing it into a thermoset epoxy resin. Composites loaded with other fillers were also prepared to evaluate their effectiveness on the mechanical properties of epoxy resin.

The tensile results are shown in Figure 3 and details of the results are summarized in Table 2. For neat epoxy resin, its average Young's modulus (E_Y), tensile strength (σ_s) and fracture toughness (G) are 1.36 GPa, 51.0, and 1.81 MPa $m^{1/2}$, respectively. The addition of 0.1 wt % GO leads to a little

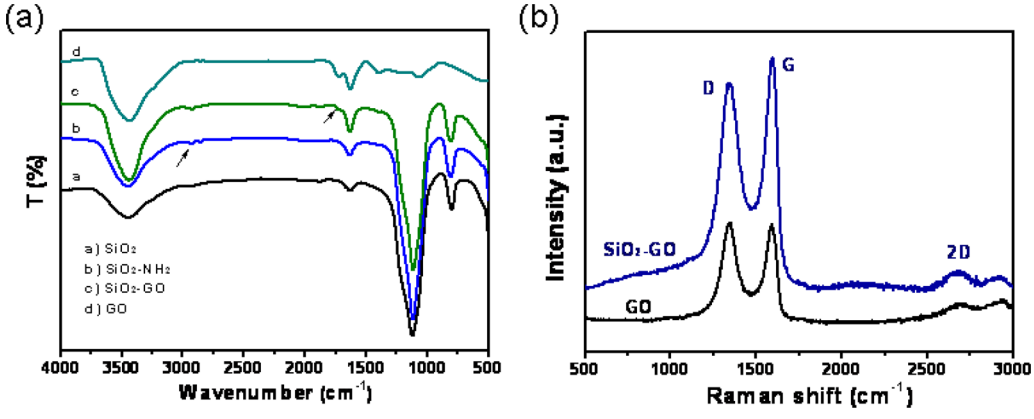

Figure 2. (a) FT-IR spectra curves of pristine SiO_2, SiO_2−NH_2, SiO_2−GO, and GO; (b) Raman spectra of GO and SiO_2−GO hybrid.

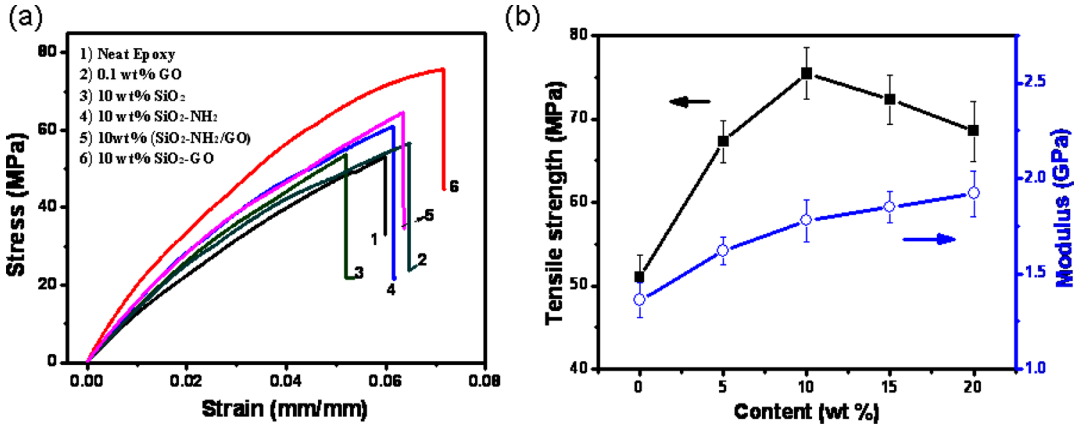

Figure 3. (a) Stress–strain curves for neat epoxy and epoxy composites; (b) effect of SiO_2–GO content on the tensile strength and modulus of epoxy resins.

Table 2. Properties of Neat Epoxy and Epoxy Composites from Tensile and DMA Test

samples	E_Y (GPa)	σ_s (MPa)	ε (%)	ε_s(MPa $m^{1/2}$)	T_g (°C)
neat EP	1.36 ± 0.09	51.0 ± 3.2	6.14 ± 0.32	1.81 ± 0.06	197.1
0.1 wt % GO	1.45 ± 0.07	59.1 ± 2.1	6.51 ± 0.16	2.16 ± 0.09	194.4
5 wt % SiO_2–GO	1.62 ± 0.07	67.3 ± 2.5	6.77 ± 0.18	2.78 ± 0.08	201.3
10 wt % SiO_2–GO	1.79 ± 0.11	78.5 ± 2.7	7.36 ± 0.38	3.42 ± 0.19	203.6
15 wt % SiO_2–GO	1.86 ± 0.08	72.3 ± 3.0	6.42 ± 0.24	2.91 ± 0.17	195.2
20 wt % SiO_2–GO	1.92 ± 0.15	68.5 ± 3.6	4.92 ± 0.31	1.94 ± 0.16	181.5
10 wt % SiO_2	1.54 ± 0.13	57.6 ± 3.2	4.95 ± 0.42	1.58 ± 0.14	209.1
10 wt % SiO_2–NH_2	1.62 ± 0.14	64.3 ± 4.3	6.35 ± 0.21	2.35 ± 0.11	207.8
10 wt %(SiO_2–NH_2/GO)	1.67 ± 0.11	66.5 ± 2.6	6.51 ± 0.27	2.46 ± 0.13	202.5

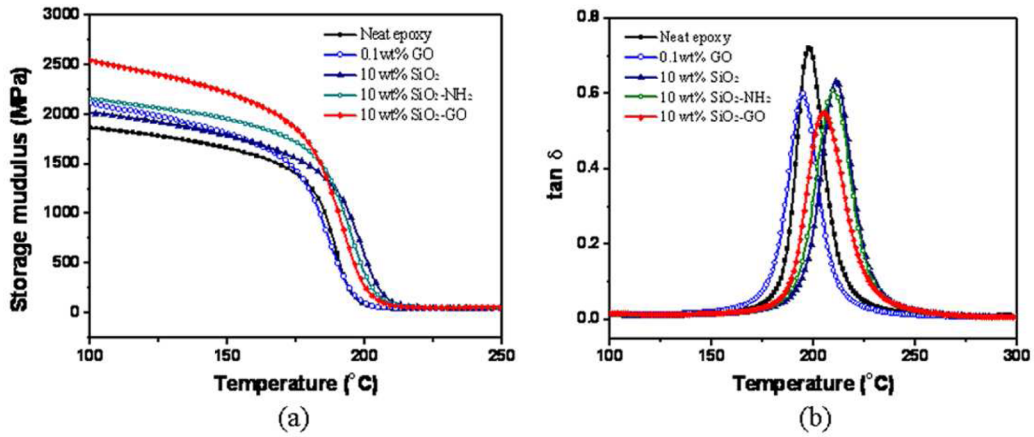

Figure 4. Plots of dynamic mechanical curves for neat epoxy and epoxy composites: (a) storage modulus; (b) damping spectra (tan δ).

increase of epoxy composites tensile modulus and strength. Composites loaded with silica particles with different surface properties show quite different mechanical behavior. The incorporation of 10 wt % pristine SiO_2 results in a moderately improved tensile modulus and strength of epoxy composites, with average values of 1.54 GPa and 57.6 MPa, respectively. The elongation at break of the composites is decreased and the fracture toughness also slightly reduced to 1.58 MPa $m^{1/2}$. The composites loaded with 10 wt % SiO_2–NH_2 and SiO_2–GO show simultaneously improved stiffness and toughness, and the improvement was more remarkable for SiO_2–GO, whose average values of E_Y,σ_s, and G greatly increased to 1.79 GPa, 78.5 MPa, and 3.42 MPa $m^{1/2}$, respectively. That is 8.5, 22.1, and 45.3% increases compared with composites loaded with SiO_2–NH_2. Moreover, ternary composites containing 10 wt % SiO_2–NH_2 and 0.1% GO (the same contents with 10 wt % SiO_2–GO) were also prepared by simply dispersing the two particles in epoxy matrix, which possessed only very limited mechanical improvement compared with that of composites with 10 wt % SiO_2–NH_2 loading. It suggests that the mechanical enhancement effect of SiO_2–GO hybrid is caused by the presence of the GO shells on the silica surface, and the optimal placement of the GO additives is right at the silica/matrix interface for maximum effectiveness.

Composites loaded with different content of SiO_2–GO hybrid were also studied. As shown in Figure 3(b) and Table 2, in the range of 5 to 20 wt % loading, the addition of SiO_2–GO hybrid leads to an effective enhancement of tensile modulus,

dx.doi.org/10.1021/am3010576 | ACS Appl. Mater. Interfaces 2012, 4, 4398–4404

strength and fracture toughness of epoxy composites at all fillers loadings. Composites loaded with 10 wt % SiO_2−GO exhibited optimum reinforcement effect, further increase of SiO_2−GO led to a continuous increase of modulus, whereas the tensile strength, elongation at break and fracture toughness decreased concurrently. Compared with neat epoxy resin, the incorperation of 10 wt % of SiO_2−GO improved the ultimate tensile strength, tensile strain and toughness by a factor of 31.6, 53.9, and 100%, respectively. When compared with existing literatures concerning the mechanical reinforcement of epoxy resin,[34−39] the mechanical reinforcement by the submicro sized silica reported here is also very remarkable.

3.3. Dynamic Mechanical Behavior. The mechanical properties of the epoxy composites is also evaluated using dynamic mechanical analysis (DMA), which is considered as a convincing approach to illustrate the interaction between the fillers and matrix.[40,41]

Figure 4a presents the storage modulus curves of the neat epoxy and epoxy composites. Overall, the storage modulus of epoxy composites increases with the addition of all types of fillers. In the initial glassy state, the composites loaded with 10 wt % SiO_2−GO hybrid exhibited an enhanced storage modulus to pure epoxy polymer and that of other composites. For example, at the temperature of 100 °C, the storage modulus of composites containing 10 wt % SiO_2−GO is 2.58 GPa, which is 41.7% larger than that of neat epoxy resin (1.82 GPa) as well as 15.5% larger than that of composites loaded with 10 wt % SiO_2−NH_2 (2.24 GPa). The enhanced storage modulus indicates that in the glassy state, the motion of epoxy matrix chains is restricted by the filler and the SiO_2−GO hybrids have stronger interfacial adhesion with the matrix in comparison with other fillers. However, as the temperature approches to T_g, the storage modulus of the composites loaded with SiO_2−GO decreased sharply, even lower than composites loaded with SiO_2 or SiO_2−NH_2.

To understand the sharp decrease of the storage modulus of composites loaded with SiO_2−GO, the DMA curves of the tan δ versus temperature are presented in Figure 4b, the glass transition temperatures (T_g) extracted in term of the peak temperature of the curves are also listed in Table 1. The T_g occurs at 197 °C for pure epoxy resin, whereas it slightly shifts to lower temperature (194.4 °C) for composites loaded with 0.1 wt % of GO. For composites loaded with 10 wt % SiO_2, the T_g increased to 209.1 °C, that is nearly 12 °C higher than that of neat epoxy resin. While, composites loaded with the same content of reactive SiO_2−NH_2 and SiO_2−GO lead to 10.7 and 6.5 °C increase of T_g values, which are lower than that of composites loaded with SiO_2 particles. This contradicts the typical confined relaxation behavior in polymer composites, where an increase of T_g is generally observed for covalently bonded interface interactions. For composites loaded with GO that contains abundant reactive groups, the reaction between GO and amine curing agent should easily occur during the curing process.[20] This interfacial reaction leads to stronger interfacial interactions with epoxy resin, on the other hand, it can change the stoichiometry and microstructure of the network at the epoxy/GO interface.[42,43]As a result, the GO highly influences the molecular dynamics and cross-linking density of the epoxy matrix, thereby increasing the storage modulus and reducing the T_g of the composites. With this in mind, it is clear that the extra reactive groups of GO on the hybrid could also change the molar ratio of epoxy to amine groups. The relatively reduced T_g values thus can be ascribed to the reduced network density. Previous studies revealed that the changes T_g of epoxy composites could be attributed to the synergy of network density and particle confinement.[35,42,43] In the present study, there exist two competing factors, that is the confinement of the filler−matrix interface and the reduction in organic network density, dominate the relaxation behavior of epoxy segments.

3.4. Structural Characterization of Epoxy Composites. To get more information about the interfacial interaction between the matrix and silica fillers, we investigated the fracture microstructure of samples loaded with 10 wt % of the three types of silica fillers by SEM.

For composites loaded with SiO_2, the fractograph is rather smooth with some stripe structures (Figure 5a), some SiO_2 agglomerates are observed, debonded SiO_2 particles are visible as denoted by red arrows and in the amplified image. For epoxy/SiO_2−NH_2 composites (Figure 5c,d), the silica particles are well-embedded in the epoxy matrix with stronger interfaces, where the debonded particles can hardly be observed. On the other hand, composites loaded with SiO_2−GO exhibit a rough fracture surface, where the shape of the ribbons becomes irregular and evolves into smaller fragments, the cracks appear in some deeper places on the fracture surface, and the silica microspheres can be hardly seen from the low magnification image. This implies that the SiO_2−GO surfaces are most likely coated by a layer of the epoxy resin. The indentations and rough fractograph are originated from the pulling-out of resin-coated SiO_2−GO when the load goes beyond the strength limit of the flexible interphase. The hybrid particles have inhibited

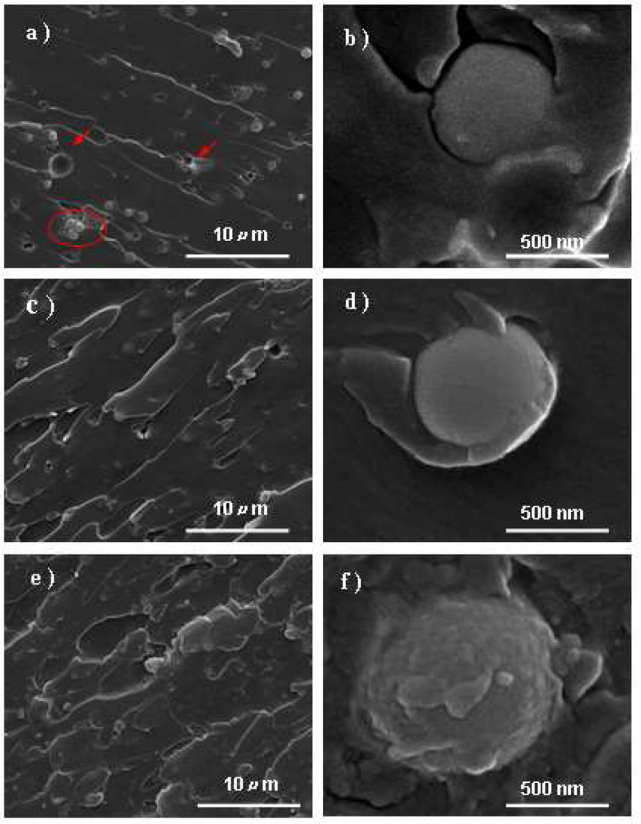

Figure 5. SEM images of fractured surface (a, b) composites loaded with 10 wt % SiO_2 (c, d), SiO_2−NH_2, and (e, f) SiO_2−GO, at low and high magnifications, respectively.

the propagation of cracks and slowed down the advancing of the crack front more effectively, leading to the significant toughening effect. All these observations are in good agreement with the tensile properties results.

3.5. Reinforcement Mechanism of SiO_2–GO and Outlooks. The optimization of the interfacial adhesion has been a subject of numerous studies for the preparation of epoxy/silica composites. Silane coupling agents treatment provides a simple and effective way to substituting the silica silanol groups into other functional groups.[8,44,45] These reactive groups can copolymerize with the epoxy matrix monomers, and thus covalently incorporate the silica into the matrix, whereas it seems that the tightly coated GO shells on the silica surface are more effective than the commonly used coupling agent APS for the modification of silica surfaces and for the composites mechanical properties enhancement. This is likely due to the fact that abundant functional groups of the GO provide more chances to react with the epoxy components during the curing process, and the two-dimensional structure of GO shells could also provide a perfect template for the forming of the grafting layer on the silica surface. The presence of a soft coating of self-propagated linkages among epoxy and the hybrid also creates a network with lower cross-link density at the interface region, which may also cause an additional increase in toughness due to the formation of a looser, more mobile network that is able to absorb energy more efficiently than a highly cross-link network.[42,46] Moreover, the roughness surface and wrinkled surface topology of the hybrid (Figure.1 b) may also enable it to mechanically interlock with the epoxy chains far more effectively than the smooth silica microspheres.[47]

Polymer/silica composites have attracted substantial academic and industrial interest recent years.[48]The present work explores the possibility to improve epoxy–silica interfacial interaction and structure by wrapping silica with GO shells. Different from the traditional application of GO used as a polymer nanofiller, the GO shells on the silica surface served as a unconventional coupling agent in this system, which greatly improved the interfacial strength between SiO_2 and the epoxy matrix. The unique two-dimensional structure and abundant functional groups make GO more effective than the commonly used silane coupling agent for the modification of silica surface, which in turn strongly affect the polymer composite properties. The concept of using GO as fillers surface modifier can be also applied to the treatment of many other inorganic particles, suggesting a broad application in the development of advanced polymer composites.

4. CONCLUSION

We have demonstrated that GO coating on silica particle can largely enhance the mechanical properties of epoxy/silica composites. Located at the epoxy–silica interface, the GO shells on silica surface could serve as a potent coupling agent for the modification of silica particles, leading to a great enhancement of interfacial interactions and mechanical reinforcement for epoxy/silica composites. The concept of using GO as a novel coupling agent provides a powerful way to control composites interfacial structure and properties. This new and effective approach may open up opportunities to develop various high-performance composite materials with good potential in industrial applications.

AUTHOR INFORMATION

Corresponding Author

*Tel: +86-28-85461795 (Q.F.); +86 28 8546 0690 (F.C.). E-mail: qiangfu@scu.edu.cn (Q.F.). fengchen@scu.edu.cn (F.C.).

Notes

The authors declare no competing financial interest.

ACKNOWLEDGMENTS

We express our great thanks to the National Natural Science Foundation of China for financial support (51121001, 51103090, and 50973068). This work was subsidized by Guangdong Shengyi Technology Limited Corporation (China).

REFERENCES

(1) Gomez-Romero, P. *Adv. Mater.* **2001**, *13*, 163–174.
(2) Sanchez, C.; Julián, B.; Belleville, P.; Popall, M. *J. Mater. Chem.* **2005**, *15*, 3559–3592.
(3) Mammeri, F.; Le Bourhis, E.; Rozes, L.; Sanchez, C. *J. Mater. Chem.* **2005**, *15*, 3787–3811.
(4) Jancara, J.; Douglasc, J. F.; Starrf, F. W.; Kumard, S. K.; Cassagnaue, P.; Lesserg, A. J.; Sternsteinh, S, S.; Buehler, M. J. *Polymer* **2010**, *51*, 3321–3343.
(5) Sun, Y. Y.; Zhang, Z. Q.; Wong, C. P. *Polymer* **2005**, *46* (7), 2297–2305.
(6) Liu, Y. L.; Lin, Y. L.; Chen, C. P.; Jeng, R. J. *J. Appl. Polym. Sci.* **2003**, *90*, 4047–4053.
(7) Ahmad, F. N.; Jaafar, M.; Palaniandy, S.; Azizli, K. A. *Compos. Sci. Technol.* **2008**, *68* (2), 346–353.
(8) Bugnicourt, E.; Gérard, J. F.; Barthel, H. *Polymer* **2007**, *48*, 1596–1605.
(9) Schadler, L. S.; Kumar, S. K.; Benicewicz, B. C.; Lewis, S. L.; Harton, S. E. *MRS Bull.* **2007**, *32*, 335–340.
(10) Liu, Y. L.; Hsu, C. Y.; Wang, M. L.; Che, H. S. *Nanotechnology* **2003**, *14*, 813–819.
(11) Zhang, X. Q.; Fan, X. Y.; Chun, Y.; Li, H. Z.; Zhu, Y. D.; Li, X. T.; Yu, L. P. *ACS Appl. Mater. Interfaces* **2012**, *4*, 1543–1552.
(12) Zhu, J.; Peng, H.; Macias, F. R.; Margrave, J. L.; Khabashesku, V. N.; Imam, A. M.; Lozano, K.; Barrera, E. V. *Adv. Funct. Mater.* **2004**, *14*, 643–648.
(13) Liu, K.; Chen, L.; Chen, Y.; Wu, J. L.; Zhang, W. Y.; Chen, F.; Fu, Q. *J. Mater. Chem.* **2011**, *21*, 8612–8617.
(14) Hummers, W. S.; Offeman, R. E. *J. Am. Chem. Soc.* **1958**, *80* (6), 1339.
(15) Park, S.; Ruoff, R. *Nat. Nanotechnol.* **2009**, *4* (4), 217–224.
(16) Dreyer, D. R.; Park, S.; Bielawski, C. W.; Ruoff, R. S. *Chem. Soc. Rev.* **2010**, *39*, 228–240.
(17) Zhu, Y.; Murali, S.; Cai, W.; Li, X.; Suk, J. W.; Potts, J. R.; Ruoff, R. S. *Adv. Mater.* **2010**, *22*, 3906–3924.
(18) Ramanathan, T.; Abdala., A. A.; Stankovich, S.; Dikin, D. A.; Herrera-Alonso, M.; Piner, R. D.; Adamson, D. H.; Schniepp, H. C.; Chen, X.; Ruoff, R. S.; Nguyen, S. T.; Aksay, I. A.; Prud'homme, R. K.; Brinson, L. C. *Nat. Nanotechnol.* **2008**, *3*, 327–331.
(19) Cai, D.; Song, M. *J. Mater. Chem.* **2010**, *20*, 7906–7915.
(20) Yang, H.; Shan, C.; Li, F.; Zhang, Q.; Han, D.; Niu, L. *J. Mater. Chem.* **2009**, *19*, 8856–8860.
(21) Kim, J.; Cote, L. J.; Kim, F; Yuan, W.; Shull, K. R.; Huang, J. X. *J. Am. Chem. Soc.* **2010**, *132*, 8180–8186.
(22) Xu, Y. X.; Shi, G. Q. *J. Mater. Chem.* **2011**, *21*, 3311–3323.
(23) Vickery, J. L.; Patil, A. J.; Mann, S. *Adv. Mater.* **2009**, *21*, 2180–2184.
(24) Han, T. H.; Lee, W. J.; Lee, D. H.; Kim, J. E.; Choi, E. Y.; Kim, S. O. *Adv. Mater.* **2010**, *22*, 2060–2064.
(25) Yang, S.; Feng, X.; Yang, I. S.; Müllen, K. *Angew. Chem., Int. Ed.* **2010**, *49*, 8408–8011.
(26) Akhavan, O.; Ghaderi, E.; Esfandiar, A. *J. Phys. Chem. B* **2011**, *115*, 6279–6288.

(27) Wang, S.; Manga, K. K.; Zhao, M.; Bao, Q.; Loh, K. P. *Small* **2011**, *7*, 2372−2378.
(28) Ling, X.; Xie, L. M.; Fang, Y.; Xu, H.; Zhang, H.; Kong, J.; Dresselhaus, M. S.; Zhang, J.; Liu, Z. *Nano Lett.* **2010**, *10*, 553−561.
(29) Xu, C.; Wang, X. *Small* **2009**, *5*, 2212−2217.
(30) Lee, J.; Novoselov, K. S.; Shin, H. S. *ACS Nano* **2011**, *5*, 608−612.
(31) Calizo, I.; Balandin, A. A.; Bao, W.; Miao, F.; Lau, C. N. *Nano Lett.* **2007**, *7*, 2645−2649.
(32) Ferrari1, A. C.; Meyer, J. C.; Scardaci1, V.; Casiraghi1, C.; Lazzeri, M.; Mauri, F.; Piscanec1, S.; Jiang, D.; Novoselov, K. S.; Roth, S.; Geim, A. K. *Phys. Rev. Lett.* **2006**, *97*, 187401.
(33) Kim, K. S.; Zhao, Y.; Jang, H; Lee, S. Y.; Kim, J. M.; Kim, K. S.; Ahn, J. H.; Kim, P.; Choi, J. Y.; Hong, B. H. *Nature* **2009**, *457*, 706−710.
(34) Liang, Y. L.; Pearson, R. A. *Polymer* **2009**, *50*, 4895−4905.
(35) Zhu, J.; Peng, H.; Macias, F. R.; Margrave, J. L.; Khabashesku, V. N.; Imam, A. M.; Lozano, K.; Barrera, E. V. *Adv. Funct. Mater.* **2004**, *14*, 643−648.
(36) Ma, J.; Mo, M. S.; Du, X. S.; Rosso, P.; Friedrich, K.; Kuan, H. C. *Polymer* **2008**, *49* (16), 3510−3523.
(37) Sun, D. Z.; Chu, C. C.; Sue, H. J. *Chem. Mater.* **2010**, *22*, 3773−3778.
(38) Ragosta, G.; Abbate, M.; Musto, P.; Scarinzi, G.; Masci, L. *Polymer* **2005**, *46*, 10506−10516.
(39) Liu, J.; Thompson, Z. J.; Sue, H. J.; Bate, F. S.; Hillmyer, M. A.; Dettloff, M.; Jacob, G.; Verghese, N.; Pham, H. *Macromolecules* **2010**, *43*, 7238−7243.
(40) Pan, Y. Z.; Xu, Y.; An, L.; Lu, H. B.; Yang, Y. L.; Chen, W.; Nutt, S. *Macromolecules* **2008**, *41*, 9245−9258.
(41) Lu, H. B.; Shen, H. B.; Song, Z. L.; Shing, K. S.; Tao, W.; Nutt, S. *Macromol. Rapid Commun.* **2005**, *26*, 1445−1450.
(42) Fang, M.; Zhang, Z.; Li, J. F.; Zhang, H. D.; Lu, H. B.; Yang, Y. L. *J. Mater. Chem.* **2010**, *20*, 9635−9643.
(43) Bao, C. L.; Guo, Y. Q.; Song, L.; Kan, Y. C.; Qian, X. D.; Hu, Y. *J. Mater. Chem.* **2011**, *21*, 13290−13298.
(44) Vejayakumaran, P.; Rahman, I. A.; Sipaut, C. S.; Ismail, J.; Chee, C. K. *J. Colloid Interface Sci.* **2008**, *328*, 81−91.
(45) Liu, Y. L.; Hsu, C. Y.; Wang, M. L.; Chen, H. S. *Nanotechnology* **2003**, *14*, 813−819.
(46) Putz, K. W.; Palmeri, M. J.; Cohn, R. B.; Andrews, R.; Brinson, L. C. *Macromolecules* **2008**, *41*, 6752−6756.
(47) Ganesan, Y.; Peng, C.; Lu, Y.; Loy, P. E.; Moloney, P.; Barrera, E.; Yakobson, B. I.; Tour, J. M.; Ballarini, R.; Lou, J. *ACS Appl. Mater. Interfaces* **2011**, 3 (2), 129−134.
(48) Zou, H.; Wu, S. S.; Shen, J. *Chem. Rev.* **2008**, *108*, 3893−3857.